

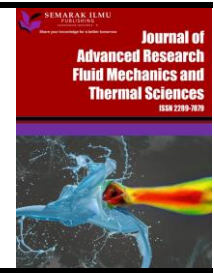


Journal of Advanced Research in Fluid Mechanics and Thermal Sciences

Journal homepage:

https://semarakilmu.com.my/journals/index.php/fluid_mechanics_thermal_sciences/index

ISSN: 2289-7879



Features of MHD on Secant Curved Annular Circular Plate Lubricant as a Couple-Stress Fluid with Slip Velocity

Ramesh Sadanand Kempepatil¹, Ayyappa Gundayya Hiremath², Jagadish Patil^{3,*}, Hanumagowda Bannihalli Naganagowda⁴, Mangala Kandagal¹, Fateh Mebarek-Oudina⁵

¹ Department of Mathematics, Faculty of Science and Technology, Sharnbasva University, Kalaburagi, 585102, India

² Department of Mathematics, Poojya Doddappa Appa College of Engineering, Kalaburagi 585102, India

³ Department of Mathematics, School of Applied Sciences, REVA University, Bangalore 560064, India

⁴ Department of Mathematics, Faculty of Engineering and Technology, Sharnbasva University, Kalaburagi, 585102, India

⁵ Department of Physics, Faculty of 20 août 1955-Skikda, Skikda, Algeria

ARTICLE INFO

ABSTRACT

Article history:

Received 9 May 2024

Received in revised form 30 August 2024

Accepted 15 September 2024

Available online 30 September 2024

Keywords:

MHD; slip velocity; curved annular circular plate; Reynolds Equation; lower curvature; upper curvature

The purpose of this study is to examine the magneto-hydrodynamic (MHD) and slip velocity effect on secant curved annular circular plates lubricated with couple stress fluid and to derive the modified Reynolds's equation for non-Newtonian fluid under various operating conditions to obtain the optimum bearing parameters. Based upon the MHD theory and Stokes theory for couple stress fluid, the governing equations relevant to the problem under consideration are derived. This paper analyses the effect of slip velocity on secant curved annular circular plates with an electrically conducting fluid in the presence of a transverse magnetic field. It is found that there is an increase in squeeze film pressure, load carrying capacity and squeeze film time in secant curved annular circular plates due to the presence of magnetic effects with couple stress fluid and slip velocity.

1. Introduction

Nowadays, several engineering and industrial applications rely on flow analysis based on magneto-hydrodynamics (MHD). Over their conventional counterparts, MHD bearings that use conducting fluids have superior electrical and thermal conductivity. Polymer technology, accelerators, electrostatic precipitation, the petroleum industry, fluid droplets, MHD pumps, crude oil purification, and power generators are just a few of the many areas that have found use for MHD flow. After looking at the MHD journal bearing, Kuzma *et al.*, [1] found that using a magnetic field increased the bearing load-carrying capability. Maki *et al.*, [2] flow between parallel plates was investigated. Many researchers have been examined in presence of a magnetic field. Bujurke and Kudenatti [3], Lin [4], Kudenatti *et al.*, [5], Singh and Sharma [6], and Zhao *et al.*, [7], alterations in

* Corresponding author.

E-mail address: jagadish_patil@sharnbasvauniversity.edu.in

<https://doi.org/10.37934/arfmts.121.2.201215>

the properties of bearings lubricated with electrically conduction fluid. They observed as magnetic field increased capacity to bearing weight.

All of these studies are conducted with the lubricant treated as a Newtonian fluid in accordance with the classical hydrodynamic theory of lubrication. Applying this prediction to engineering challenges renders it invalid. The use of minute additives to boost fluid viscosity greatly facilitated the development of advanced machines. Additives usually consist of long-chained polymers, granular material, or suspensions. As the most basic standard theory of fluids, Stokes [8] micro continuum hypothesis examines polar collision and provides a detailed explanation of the non-Newtonian fluids' peculiar behavior. The idea behind couple stress fluids is that the distribution of momentum and force is the same as the interaction of one body component with another across a surface. Many authors studied effect of couple stress [9,10]. Compared with conventional bearings, those that use MHD and conducting fluids provide plenty of advantages.

Samylingam *et al.*, [11] discussed the enhancing lubrication efficiency and wear resistance in mechanical systems through the nano fluids. Ideris *et al.*, [12] made the analysis of coating and lubrication on friction and wear for metal to metal application. Ismail *et al.*, [13] experimental investigation on Newtonian behavior and viscosity of TiO₂/PVE Nano lubricants for applications in refrigeration. Huo *et al.*, [14] and Ghabussi *et al.*, [15] studied bending analysis of FG-GPLRC axisymmetric circular /annular sector plates by considering elastic foundation and horizontal friction force using 3D poroelasticity, and seismic performance of cold formed and hot rolled steel wall system equipped with curved steel dampers. Zhang *et al.*, [16] studied on Low velocity impact resonance of FG-GPLRC viscoelastic doubly curved panel. Al-Furjan *et al.*, [17] studied on non-polynomial frame work for stress and strain response of the FG-GPLRC disk using 3 dimensional refined higher order theory. Safapour *et al.*, [18] done the analysis on frequency characteristics of FG-GPLRC viscoelastic thick annular with the aid of GDQM Thin walled.

It is necessary to study about the combined impact of MHD couple stress lubrication because it has lot of applications in bearing systems. Many researchers have made an investigation on MHD couple stress lubrication theory [19-22]. Studies combined effect of MHD couple stress and viscosity variation by Suresha *et al.*, [23] and MHD couple stress effects on infinitely wide slider and infinitely tube endoscope bearings. Devakar *et al.*, [24], Nabhani and El Khelifi [25], and Sahraoui and Kaviany [26] discussed effect of slip velocity on porous plane media. Ahmad and Singh [27] resulted on porous-pivoted slider bearings with slip velocity. Yang *et al.*, [28], Shah and Bhat [29], Guo *et al.*, [30], and Ahmad and Singh [31] investigated lubrication with slip velocity effect. Recently, Jayaprakash *et al.*, [32] made the analysis on influence of MHD and couple stress on curved circular and porous-rough flat plate, from this study author demonstrate that, MHD and couple stress boost the pressure, load support and squeezing time compared to Newtonian and non-magnetic cases. The effect of permeability of the porous layer is to decrease the load carrying capacity as it gives an easy path for the lubricant to pass through. Cyriac *et al.*, [33] elaborated the impacts of MHD couple stress on rough secant slider bearings, from this study we noted that the bearing features increase with the longitudinal roughness parameter, and the reverse phenomenon is observed with the transverse roughness parameter. When transverse roughness pattern is assumed on a secant slider bearing, characteristics like pressure, load, stiffness of the film, and damping coefficient increases significantly. Vinutha *et al.*, [34] studied on long cylinder and infinite Rough Plate with slip velocity. We gone through these studies and got the information about the use of MHD couple stress lubricants will improve the bearing capacity.

From the literature review, no study has been carried out on this topic. So, in this article we made theoretical study of MHD slip velocity and couple stress lubricants effects on secant curved annular circular plate.

2. Methodology and Mathematical Solution

The geometry of secant curved annular circular plate is shown in Figure 1(a) and Figure 1(b). In Figure 1(a), b is the internal radius and a is the external radius. In two circular plates the lower plate is fixed and upper plate moves towards the lower plate with squeezing velocity $v = \left(-\frac{\partial h_m}{\partial t}\right)$. Here, h is thickness of the film and that can be produced by exponential function i.e.

$$h = h_m \exp(-\alpha r^2) \quad (1)$$

where h_m is minimum film thickness and r be the radial coordinate. The external magnetic field B_0 is applied to the bearing in the z -direction. It is supposed that the fluid film is thin, the body couples and the body forces are insignificant. Figure 1(b) illustrated the 3D visualization of the bearing system.

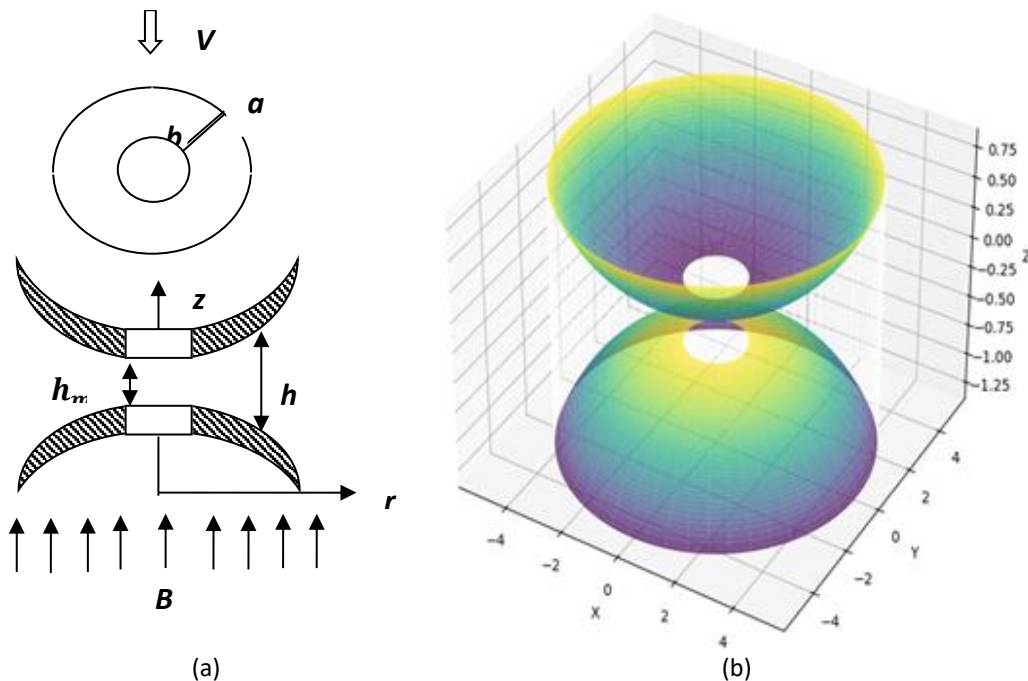


Fig. 1. (a) Geometrical representation of the problem, (b) 3D visualization of the problem

In view of these suppositions, the theory of hydrodynamic lubrication applied to the films, the equation of continuity and the MHD governing equations of motion in polar coordinate are.

$$\mu \frac{\partial^2 u}{\partial z^2} - \eta \frac{\partial^4 u}{\partial z^4} - \sigma B_0^2 u = \frac{\partial p}{\partial r} \quad (2)$$

$$\frac{\partial p}{\partial z} = 0 \quad (3)$$

$$\frac{1}{r} \left(\frac{\partial}{\partial r} \right) r u + \left(\frac{\partial v}{\partial z} \right) = 0 \quad (4)$$

The boundary conditions are

(i) At the upper plate $z = h$

$$u = 0 \quad \frac{\partial^2 u}{\partial z^2} = 0 \quad v = -\frac{\partial h_m}{\partial t} \quad (5)$$

(ii) At the lower plate $z = 0$

$$u = \frac{1}{s} \left(\frac{\partial u}{\partial z} \right)_{z=0} \quad \frac{\partial^2 u}{\partial z^2} = 0 \quad v = 0 \quad (6)$$

$$s = \frac{\alpha}{\sqrt{k}} \quad (7)$$

where, s be the slip velocity.

The velocity u is gained by solving (2) using (5), (6) and (7) we get

$$u = \left\{ \frac{\phi_1}{\phi_2} \times \phi_3 - \phi_4 - 1 \right\} \frac{h_m^2}{\mu M_0^2} \frac{\partial p}{\partial r} \quad (8)$$

where,

$$\phi_1 = 1 - \frac{AB^2}{(A^2 - B^2)sl} \operatorname{Cosech} h \frac{Ah}{l} + \frac{BA^2}{(A^2 - B^2)sl} \operatorname{Cosech} h \frac{Bh}{l},$$

$$\phi_2 = 1 - \frac{AB^2}{(A^2 - B^2)sl} \operatorname{Coth} h \frac{Ah}{l} - \frac{BA^2}{(A^2 - B^2)sl} \operatorname{Coth} h \frac{Bh}{l}$$

$$\phi_3 = \frac{B^2}{(A^2 - B^2)} \left\{ \frac{\sinh \left(\frac{A(z-h)}{l} \right)}{\sin \frac{Ah}{l}} \right\} - \frac{A^2}{(A^2 - B^2)} \frac{\sinh \left(\frac{B(z-h)}{l} \right)}{\sin \frac{Bh}{l}}$$

and

$$\phi_4 = \frac{1}{(A^2 - B^2)} \left\{ A^2 \sin h \frac{Az}{l} \operatorname{cosech} h \frac{Ah}{l} - B^2 \sinh \frac{Bz}{l} \operatorname{Cosech} h \frac{Bh}{l} \right\}$$

Substituting u in (4) applying the boundary condition (5), (6) and (7) performing an integration over film thickness. The MHD slip velocity with couple stress which yields the Reynolds equation.

$$\frac{1}{r} \frac{\partial}{\partial r} \left\{ r f(B_0, h, l, s) \frac{\partial p}{\partial r} \right\} = \mu V \quad (9)$$

where,

$$A = \left\{ \frac{1 + (1 - 4M_0^2 l^2 / h_m^2)^{1/2}}{2} \right\}^{1/2} \quad B = \left\{ \frac{1 - (1 - 4M_0^2 l^2 / h_m^2)^{1/2}}{2} \right\}^{1/2}$$

$$f(B_0, h, l, s) = \frac{l}{(A^2 - B^2)} \left\{ \frac{\left(2 - \xi_1 \text{Coth} \frac{Ah}{l} + \xi_2 \text{Coth} \frac{Bh}{l} \right)}{\left(1 - \xi_1 \text{Coth} \frac{Ah}{l} + \xi_2 \text{Coth} \frac{Bh}{l} \right)} \right\} \times$$

$$\times \left\{ \left[\left(\frac{B^2}{A} \tanh \left(\frac{Bh}{2l} \right) - \frac{A^2}{B} \tanh \left(\frac{Bh}{2l} \right) \right) \right] + \frac{(A^2 - B^2)}{l} h \right\} \frac{1}{\sigma B_0^2}$$

$$\xi_1 = \frac{AB^2}{(A^2 - B^2)sl} \quad \text{and} \quad \xi_2 = \frac{A^2 B}{(A^2 - B^2)sl}$$

The orientation of the upper plate along the surface is defined by the relationship.

$$z_u = h_m \sec(\beta r^2); \quad 0 \leq r \leq a$$

The orientation of the lower plate along the surface is defined by the relationship

$$z_l = h_m \{ \sec(\gamma r^2) - 1 \}; \quad 0 \leq r \leq a$$

Where β and γ are the curvature parameters of the corresponding plates and h_m is the central film thickness. The film thickness $h(r)$ then,

$$h(r) = h_m \{ \sec(\beta r^2) - \sec(\gamma r^2) + 1 \}; \quad 0 \leq r \leq a$$

Introducing dimensionless parameters.

$$\bar{r} = \frac{r}{a}, \bar{h} = \frac{h}{h_0}, \bar{h}_m = \frac{h_m}{h_0}, \bar{l} = \frac{l}{h_0}, K = \beta a^2, C = \gamma a^2, \bar{P} = -\frac{h_0^3 p}{\mu a^2 V}, \bar{s} = \frac{\sigma}{h_m}$$

$$\bar{h} = \{ \sec(K \bar{r}^2) - \sec(C \bar{r}^2) + 1 \}$$

Obtained the Modified Reynolds equation after substituting the above quantities in Eq. (9)

$$\frac{1}{\bar{r}} \frac{\partial}{\partial \bar{r}} \left\{ \bar{r} f(\bar{h}, \bar{l}, M_0, \bar{s}) \frac{\partial \bar{P}}{\partial \bar{r}} \right\} = -1 \quad (10)$$

where,

$$\bar{f}(\bar{h}, \bar{l}, M_0, \bar{s}) = \frac{\bar{l}}{(\bar{A}^2 - \bar{B}^2)M_0^2} \left\{ \left[\frac{\left\{ 2 - \bar{\xi}_1 \operatorname{Coth} \frac{\bar{A}\bar{h}}{2\bar{l}} + \bar{\xi}_2 \operatorname{Coth} \frac{B\bar{h}}{2\bar{l}} \right\}}{\left(1 - \bar{\xi}_1 \operatorname{Coth} \frac{A\bar{h}}{\bar{l}} + \bar{\xi}_2 \operatorname{Coth} \frac{B\bar{h}}{\bar{l}} \right)} \right] \left(\frac{\bar{B}^2}{\bar{A}} \tanh \frac{\bar{A}\bar{h}}{2\bar{l}} - \frac{\bar{A}^2}{\bar{B}} \tanh \frac{B\bar{h}}{2\bar{l}} \right) + \frac{\bar{h}(\bar{A}^2 - \bar{B}^2)}{\bar{l}} \right\}$$

where, $\bar{\xi}_1 = \frac{\bar{A}\bar{B}^2}{(\bar{A}^2 - \bar{B}^2)\bar{s}\bar{l}}$ and $\bar{\xi}_2 = \frac{\bar{B}\bar{A}^2}{(\bar{A}^2 - \bar{B}^2)\bar{s}\bar{l}}$

and

$$\bar{A} = \sqrt{\frac{1 + (1 - 4M_0^2\bar{l}^2)^{1/2}}{2}} \quad \therefore \quad \bar{B} = \sqrt{\frac{1 - (1 - 4M_0^2\bar{l}^2)^{1/2}}{2}}$$

In order to introduce the squeeze problem, the boundary conditions are,

$$\bar{P} = 0 \quad \text{at} \quad \bar{r} = \delta = b/a \tag{11}$$

$$\bar{P} = 0 \quad \text{at} \quad \bar{r} = 1 \tag{12}$$

The non-dimension squeeze film pressure is determined from the parameters for the boundary (11) and (12) and the integration of Eq. (10) as a function of \bar{r} .

$$\bar{P} = \frac{f_2(\bar{r})f_1(1) - f_1(\bar{r})f_2(1)}{2f_2(1)} \tag{13}$$

where,

$$\text{Take } f_1(\bar{r}) = \int_{\bar{r}=\delta}^{\bar{r}} \frac{1}{f(\bar{h}, \bar{l}, M_0, \bar{s})} d\bar{r}, \quad f_2(\bar{r}) = \int_{\bar{r}=\delta}^{\bar{r}} \frac{1}{r f(\bar{h}, \bar{l}, M_0, \bar{s})} d\bar{r}$$

and

$$f_1(1) = \int_{\bar{r}=\delta}^1 \frac{1}{f(\bar{h}, \bar{l}, M_0, \bar{s})} d\bar{r}, \quad f_2(1) = \int_{\bar{r}=\delta}^1 \frac{1}{r f(\bar{h}, \bar{l}, M_0, \bar{s})} d\bar{r}$$

Integrating (13) with respect to \bar{r} between limit 0 to 1 we get a non-dimensional load carrying be obtained.

$$\bar{W} = \frac{-1}{2} \int_{\bar{r}=\delta}^1 f_1(\bar{r}) \bar{r} d\bar{r} + \frac{1}{2} \frac{f_1(1)}{f_2(1)} \int_{\bar{r}=\delta}^1 f_2(\bar{r}) \bar{r} d\bar{r} \tag{14}$$

When the minimal film thickness is considered, the dimensionless response time can be calculated by integrating the equation given above.

$$\bar{T} = \int_{\bar{h}_0}^1 \left(\frac{2f_2(1)}{f_2(1) \int_{\bar{r}=\delta}^1 f_1(\bar{r}) \bar{r} d\bar{r} - f_1(1) \int_{\bar{r}=\delta}^1 f_2(\bar{r}) \bar{r} d\bar{r}} \right) d\bar{h}_m \quad (15)$$

where, $\bar{h} = \bar{h}_m \{ \sec(K\bar{r}^2) - \sec(C\bar{r}^2) + 1 \}$

3. Results and Discussion

In this article discussed the impact of MHD couple stresses and slip velocity on secant annular circular plate. For the result we applied analytical method to the governing Eq. (2), Eq. (3) and Eq. (4) with assumed boundary conditions (5), (6) and (7) and the resultant equations are reduced to non-dimensional form ordinary differential equations further the definite integrals (13), (14) and (15) are solved numerically method to obtain the various values of Hartmann number (M_0), couple stress (\bar{l}) and curvature parameters (J, K) and slip velocity (\bar{s}) with fixed parameters.

3.1 Dimensionless Pressure Distribution

Portrayal of dimensionless pressure \bar{P} as a function of \bar{r} for distinctive values of slip velocity \bar{s} is mentioned in Figure 2 and came to know from this graph there is a grow of pressure between the plates due to impact slip velocity and also larger values of pressure is noticed in the at ($\bar{s} \rightarrow \infty$). For ensuring a better performance, it is suggested that the slip parameter must be set at the larger level. Figure 3 and Figure 4 depicts the pressure \bar{P} along \bar{r} for distinctive of slip velocity \bar{s} magnetic field M_0 and couple stress lubricant \bar{l} under fixed $J = 0.8, K = 0.8$. Use of MHD is holds the movement of fluid between the film region this gives the result of higher pressure also the influence of non-Newtonian lubricants is observed to gain higher pressure as compared in case absence of magnetic field ($M_0 = 0$) and couple stress fluid ($\bar{l} = 0$). The lubricant covering in bearings allows relative motion between the bearing's surfaces, when the surfaces are sufficiently lubricated; they adhere, preventing relative motion. Both graphs show pressure decreasing along \bar{r} . Also Figure 5 and Figure 6 displays the non-dimensional pressure \bar{P} along with \bar{r} for distinct values of lower and upper curvature and keeping the parameters $M_0 = 3, \bar{l} = 0.4$ fixed then we observed that there is enhancing of pressure for curvature parameter $J = 0.2, 0.4, 0.6$ and $K = 0.2, 0.4, 0.6$ these results increasing of upper curvature decreases the pressure due to more fluid moment further increasing lower curvature increases the pressure due to less fluid moment. 3D impact of pressure versus slip velocity and magnetic field is shown in Figure 7 from this picture explain that the larger pressure distribution in the fluid film region appeared for higher values of M_0 and \bar{s} . Because the slip velocity influences the shear stress at the boundary, which in turn affect the pressure distribution in the fluid. Higher slip velocities can affect the shear stress at the boundary, thereby influencing the pressure gradient

within the fluid. In the presence of magnetic field, the Lorentz force acts on the conducting fluid, this can alter the flow dynamic and pressure distribution.

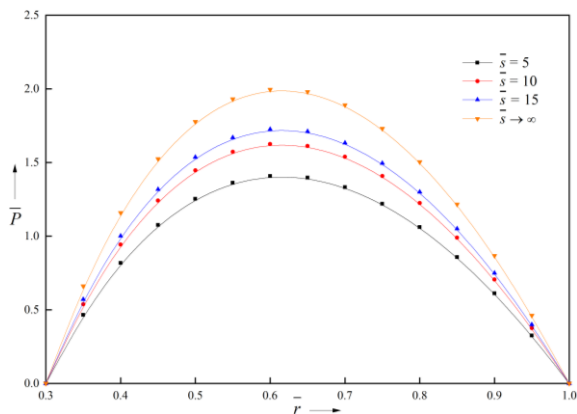


Fig. 2. Dimensionless film pressure \bar{P} versus \bar{r} for varies in \bar{s} with $\bar{l} = 0.4, J = 0.8, K = 0.8, M_0 = 3$

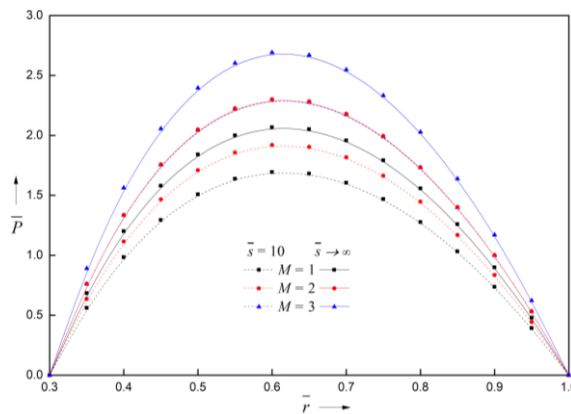


Fig. 3. Dimensionless film pressure \bar{P} versus \bar{r} for varies in M_0 with $\bar{l} = 0.4, J = 0.8, K = 0.8$

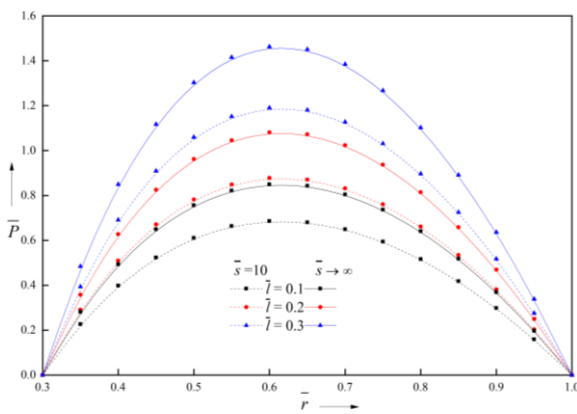


Fig. 4. Dimensionless \bar{P} versus \bar{r} for varies values of \bar{l} with $M_0 = 3, J = 0.8, K = 0.8$

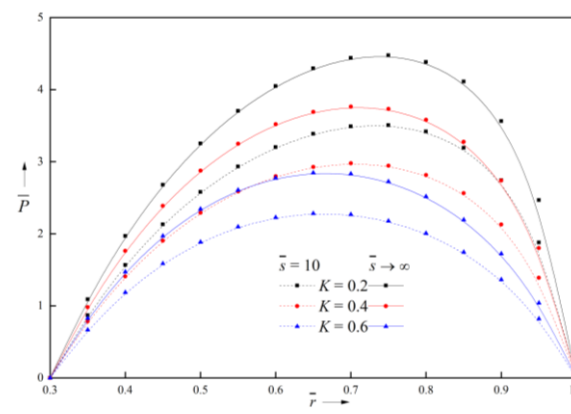


Fig. 5. Dimensionless \bar{P} versus J for various values of J with $M_0 = 3$ and $\bar{l} = 0.4$

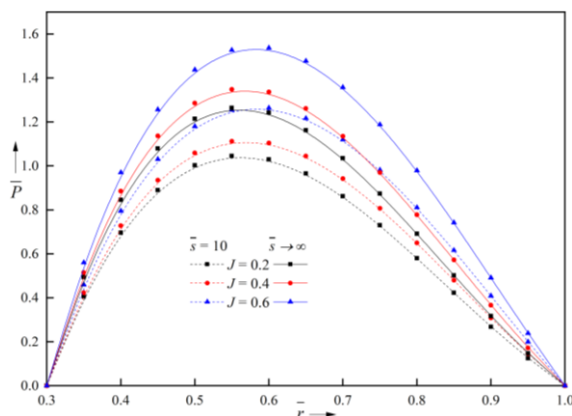


Fig. 6. Dimensionless \bar{P} versus \bar{r} for various values of J with $M_0 = 3, K = 0.8$ and $\bar{l} = 0.4$

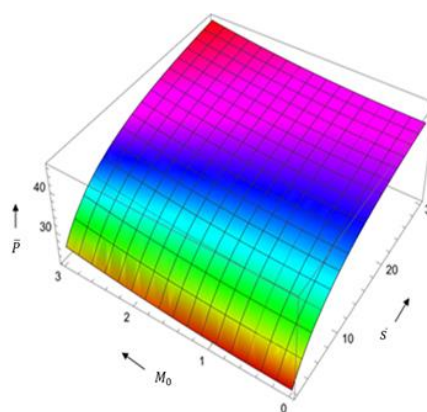


Fig. 7. 3D graph of Combined impact of Hartmann number and slip velocity on pressure

3.2 Dimensionless Load Bearing Capacity

Figure 8 describe the dimensionless \bar{W} as a function of J for different values of \bar{s} load support is noticed higher due to increase of slip velocity. Comparing with ($\bar{s} = 5,10,15$) we noticed here higher valued of load support at ($\bar{s} \rightarrow \infty$). As the slip velocity increases, the shear rates within the lubricating film also increase, which in turn generates more heat. Additionally, the film thickness between the bearing surfaces is affected, which means that the load support can be increased. Figure 9 and Figure 10 depicts \bar{W} versus J for different values of \bar{s} , M_0 and \bar{l} resulting from these graphs provides more load support especially when ($\bar{s} \rightarrow \infty$). Magnetic bearings reduce friction, maintenance and couple stress which is a materials internal resistance to deformation produced by couples or moments. Stresses and deformations in bearing components may affect load capacity. Figure 11 illustrates the effect on \bar{W} along J for different value of ($K = 0.2,0.4,0.6$) which results load capacity decreases. Further, along J increase of load due to rise of fluid moment. Figure 12 deficits that load capacity \bar{W} verses K variations of slip velocity which shows that \bar{W} is more prominent in at ($\bar{s} \rightarrow \infty$) fixed parameter $M_0 = 3, \bar{l} = 0.4$. This is due to decrease the fluid moment in larger values of slip velocity.

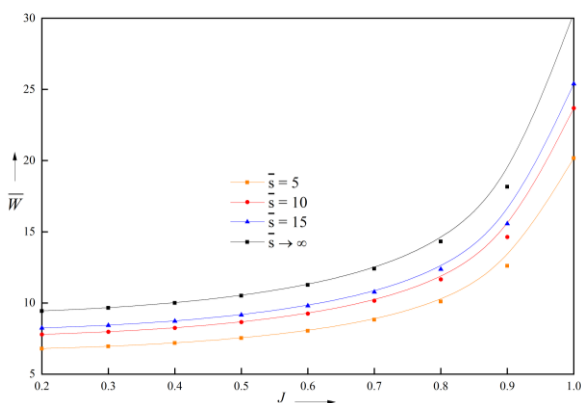


Fig. 8. Dimensionless load capacity \bar{W} verses J for various values of \bar{s} with $\bar{l} = 0.4, M_0 = 3, K = 0.8$

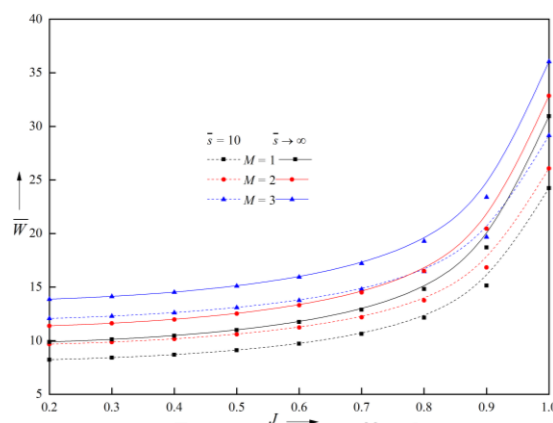


Fig. 9. Dimensionless load \bar{W} verses J for various values of M_0 with $\bar{l} = 0.4$ and $K = 0.4$

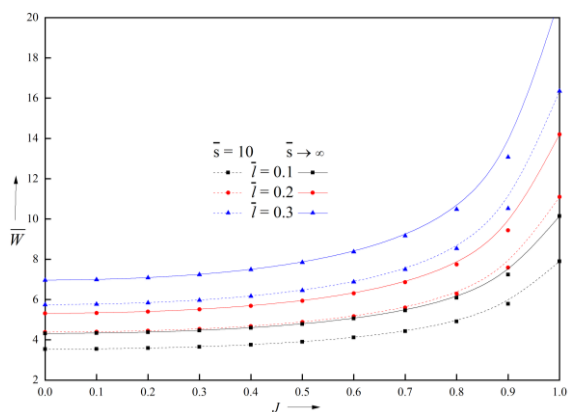


Fig. 10. Dimensionless load \bar{W} verses J for various values of \bar{l} with $M_0 = 3$ and $K = 0.8$

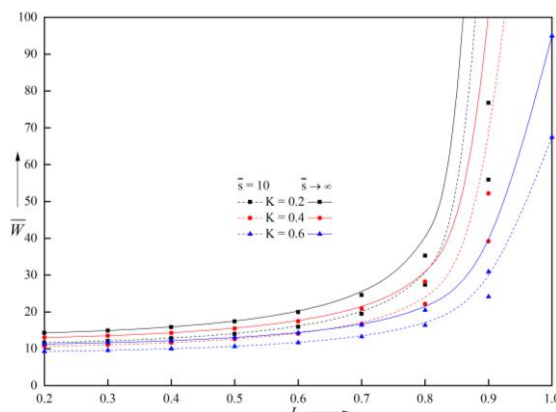


Fig. 11. Dimensionless load \bar{W} verses J for various values of K with $M_0 = 3, \bar{l} = 0.4$

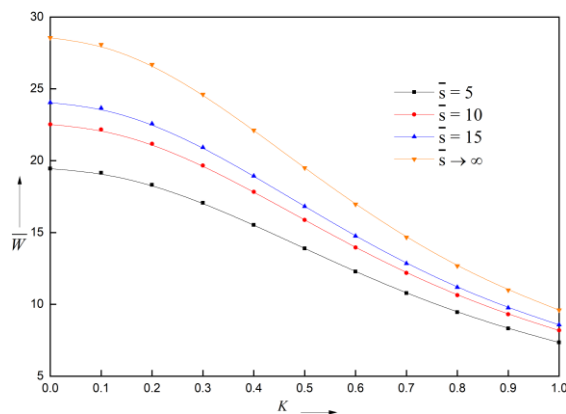


Fig. 12. Dimensionless load \bar{W} versus K for various values of \bar{s} with $M_0 = 3, \bar{l} = 0.4, J = 0.8$

Similarly in Figure 13 and Figure 14 depict that the effect of M_0 and \bar{l} on load bearing capacity \bar{W} along K observing the graphs, we can conclude that \bar{W} increases with increase in M_0 and \bar{l} from both the graph the load is more prominent in case larger values of slip velocity. Figure 15 explains the effect of lower curvature J on the load capacity along with upper curvature K and noticed here with the mounting values of J there are considerable rise in \bar{W} at $J = 0.6$. Actually, the rise of lower curvature compresses the fluid movement because generate a more pressure causes a higher load support. Furthermore, the upsurge of K decreases load also for better performance got at ($\bar{s} \rightarrow \infty$) than ($\bar{s} = 10$) with fixed parameters $M_0 = 3, \bar{l} = 0.4$.

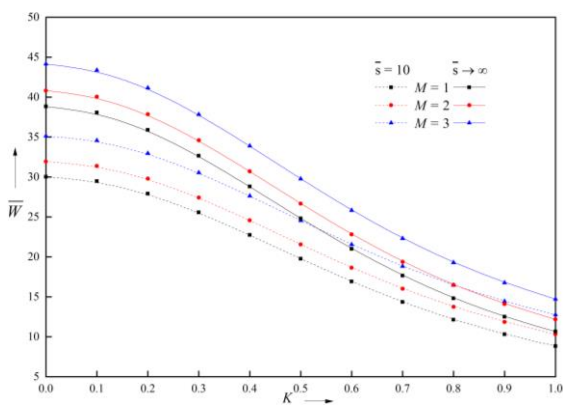


Fig. 13. Dimensionless load \bar{W} versus K for different values of M_0 with $\bar{l} = 0.4, J = 0.8$

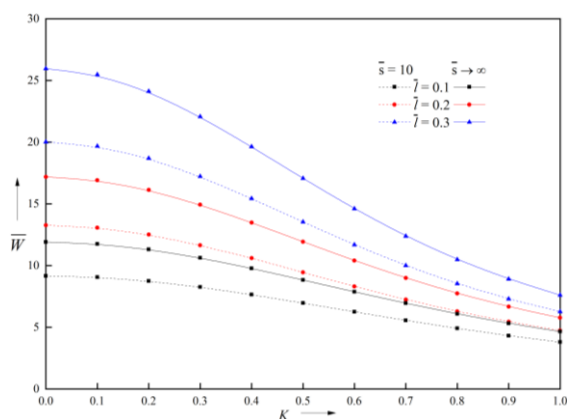


Fig. 14. Dimensionless load \bar{W} versus K for various values of \bar{l} with $M_0 = 3$ and $J = 0.8$

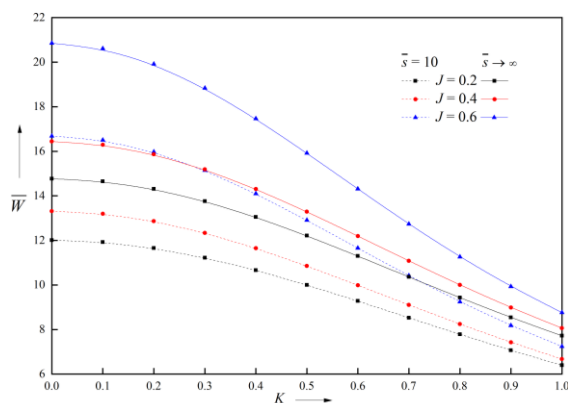


Fig. 15. Dimensionless Load \bar{W} versus K for various values of J with $M_0 = 3, \bar{l} = 0.4$

Figure 16 indicate that the 3D picture of variation of load versus slip velocity and Hartmann number which shows the boost of load support due to impact of both the parameters. Because the applied magnetic field can induce stresses within the fluid, affecting how, the fluid transmits forces across the curved plates. This can influence the structural integrity and load-bearing capabilities of the plates. Slip velocity modifies the thickness and structure of the boundary layer. This can influence the velocity profile and pressure distribution, thereby affecting the load distribution and capacity of the curved plates.

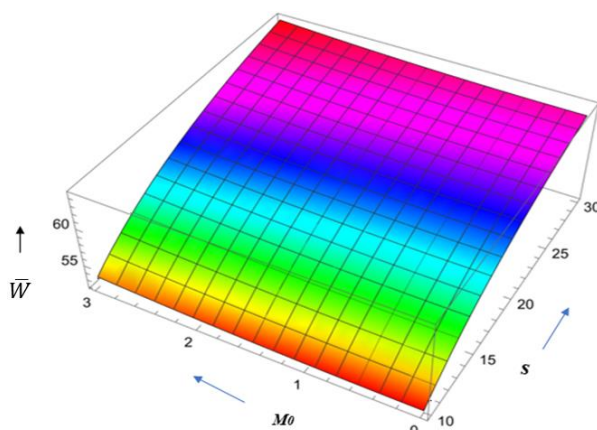


Fig. 16. 3D graph of combined impact of M_0 and \bar{s} on Load carrying capacity \bar{W}

3.3 Dimensionless Squeeze Film Time

Figure 17 illustrate the time \bar{T} versus \bar{h}_m for different values \bar{s} keeping other parameters are fixed from this graph we came to the conclusion that the higher in squeezing time for larger values of \bar{s} . The \bar{T} along \bar{h}_m for various values \bar{s} and M_0 under existence of $\bar{l} = 0.4$ and $J, K = 0.8$ are shown in Figure 18 and it is experienced that with upsurge of \bar{s} and M_0 there is gradually increase of squeeze film time. Here the solid lines indicate at $(\bar{s} \rightarrow \infty)$ it is clear to say the squeezing time larger at slip velocity $(\bar{s} \rightarrow \infty)$. Further, the magnetic properties improve the time required to squeeze a film much fluid is kept back because the flow of film material is strongly opposed by the

magnetic field squeezing becomes more time-consuming as a result. Figure 19 describes \bar{T} with \bar{h}_m for various values \bar{s} and \bar{l} with $M_0 = 3$ and $J, K = 0.8$. It is ensured that with increase of \bar{s} and \bar{l} there are considerable rise in time of response \bar{T} . From both the graph it is clear to say squeezing time reduces with increase of minimum film height \bar{h}_m in Figure 20 and Figure 21 discusses the effect of lower and upper curvature parameters effects on squeeze time \bar{T} . We discovered that squeezing time is increased with lower curvature and minimised with upper curvature. Figure 22 describes the picture of \bar{T} versus for several values of \bar{s} and M_0 on time profile it is clear to say there is an enhancement of squeezing time due to impact of \bar{s} and M_0 . Because, MHD effects reduce frictional resistance and slip velocity parameter modifies boundary conditions, both influence the squeeze film dynamics between secant curved annular circular plates by altering pressure distribution and film thickness over time.

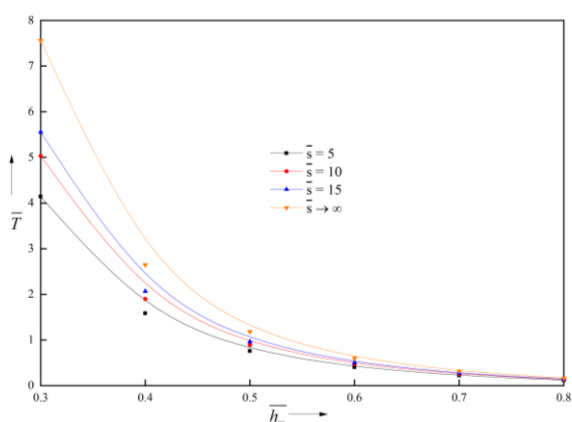


Fig. 17. Dimensionless squeezing time \bar{T} versus \bar{h}_m for different \bar{s} with $J, K = 0.8, M_0 = 3, l = 0.4$

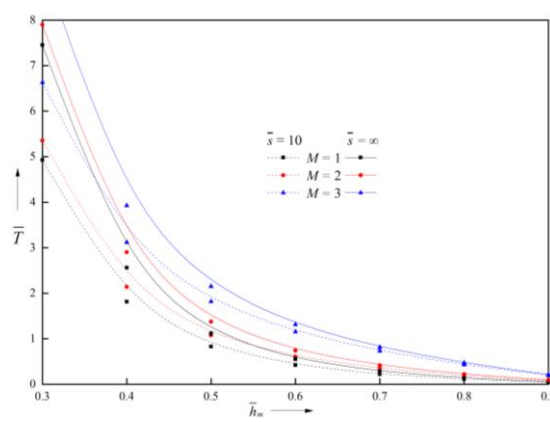


Fig. 18. Dimensionless squeezing time \bar{T} versus \bar{h}_m for different M with $J = 0.8, K = 0.8, \bar{l} = 0.4$

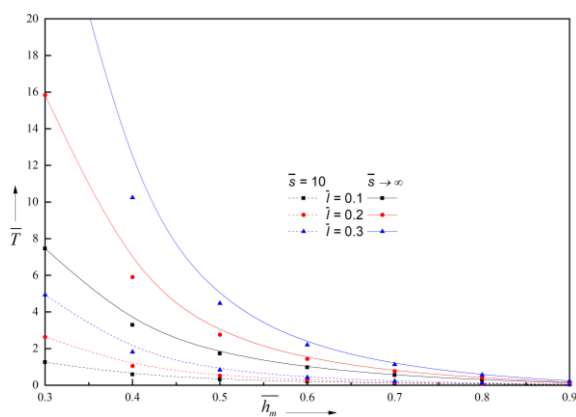


Fig. 19. Dimensionless squeezing time \bar{T} versus \bar{h}_m for different \bar{l} with $J = 0.8, K = 0.8, M_0 = 3$

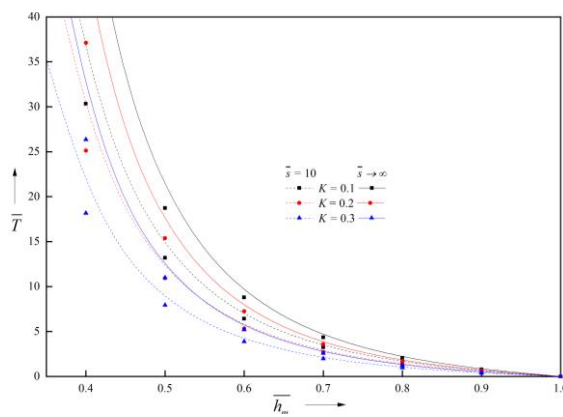


Fig. 20. Dimensionless squeezing time \bar{T} versus \bar{h}_m for different K with $J = 0.8, M_0 = 3, \bar{l} = 0.4$

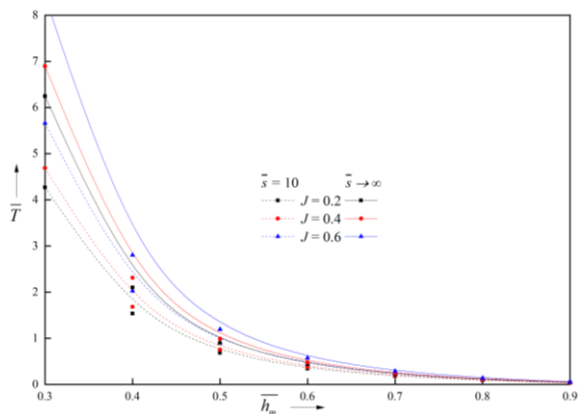


Fig. 21. Dimensionless Time \bar{T} versus \bar{h}_m for different values of J with $K = 0.8, M_0 = 3, \bar{T} = 0.4$

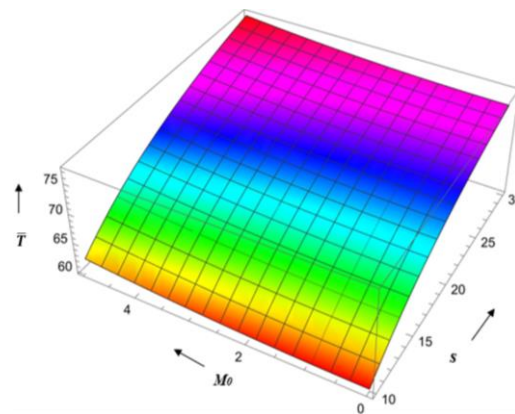


Fig. 22. 3D Graph of Combined impact of Hartmann number and slip velocity on Squeeze film time

4. Conclusions

The squeeze film performance between secant curved annular plates lubricated with couple stress fluid under the existence MHD slip velocity have been analysed in this article. According to the mathematical solution and results of discussion, the conclusion can be made as follows.

Accordance with the couple stress fluid from the Stokes theory a modified Reynolds equation is derived. Some special cases can be considered by choosing slip velocity parameter. The use of slip velocity and couple stress lubricants under the existence of Hartmann number assumes a higher in pressure distribution, load support and lengthens the squeezing time. The squeeze film attributes are more prominent at larger values of slip velocity ($\bar{s} \rightarrow \infty$) than compared to smaller values of slip velocity ($\bar{s} \rightarrow \infty$). Overall analysis it is suggested that the slip velocity parameter must be set at the larger level. These physical quantities increase bearing life and also given suitable values to improve the working of the bearing.

Designing systems that utilize MHD slip velocity with couple stress fluids require a deep understanding of the interplay between magnetic fields, fluid flow, and material properties. Engineers must account for how these factors affect the performance, stability, and reliability of the lubrication system, which can pose significant challenges.

Exploring MHD slip velocity in couple stress fluids expand our understanding of complex fluid dynamics and magneto hydrodynamics. This research can lead to new insights, theoretical developments, and practical innovations in fluid mechanics and related fields.

MHD allows for the manipulation of fluid flow through the application of a magnetic field. By adjusting the strength and orientation of the magnetic field, engineers can control the velocity distribution and shear stress within the couple stress fluid. This control can optimize the flow profile for improved performance in lubrication applications.

Acknowledgement

This research is not funded by any grants.

References

- [1] Kuzma, Dennis C., E. Roland Maki, and Russell J. Donnelly. "The magnetohydrodynamic squeeze film." *Journal of Fluid Mechanics* 19, no. 3 (1964): 395-400. <https://doi.org/10.1017/S0022112064000805>
- [2] Maki, E. Roland, Dennis C. Kuzma, and Russell J. Donnelly. "Magnetohydrodynamic lubrication flow between parallel plates." *Journal of Fluid Mechanics* 26, no. 3 (1966): 537-543. <https://doi.org/10.1017/S002211206600137X>
- [3] Bujurke, N. M., and R. B. Kudenatti. "MHD lubrication flow between rough rectangular plates." *Fluid dynamics Research* 39, no. 4 (2007): 334. <https://doi.org/10.1016/j.fluiddyn.2006.05.004>
- [4] Lin, Jaw-Ren. "MHD steady and dynamic characteristics of wide tapered-land slider bearings." *Tribology International* 43, no. 12 (2010): 2378-2383. <https://doi.org/10.1016/j.triboint.2010.07.010>
- [5] Kudenatti, Ramesh B., D. P. Basti, and N. M. Bujurke. "Numerical solution of the MHD Reynolds equation for squeeze film lubrication between two parallel surfaces." *Applied Mathematics and Computation* 218, no. 18 (2012): 9372-9382. <https://doi.org/10.1016/j.amc.2012.03.019>
- [6] Singh, Anil, and Satish C. Sharma. "Behaviour of conical porous hybrid journal bearing operated with MHD lubricant considering influence of surface irregularities." *Tribology International* 174 (2022): 107730. <https://doi.org/10.1016/j.triboint.2022.107730>
- [7] Zhao, Hui, Shuxin Fan, and Zhongwei Qu. "The Friction Performance Analysis of Textured Gear under Starved MHD Lubrication." In *Journal of Physics: Conference Series*, vol. 2610, no. 1, p. 012008. IOP Publishing, 2023. <https://doi.org/10.1088/1742-6596/2610/1/012008>
- [8] Stokes, Vijay Kumar. "Couple stresses in fluids." *Theories of Fluids with Microstructure: An Introduction* (1984): 34-80. https://doi.org/10.1007/978-3-642-82351-0_4
- [9] Naduvinamani, N. B., P. S. Hiremath, and G. Gurubasavaraj. "Squeeze film lubrication of a short porous journal bearing with couple stress fluids." *Tribology International* 34, no. 11 (2001): 739-747. [https://doi.org/10.1016/S0301-679X\(01\)00064-0](https://doi.org/10.1016/S0301-679X(01)00064-0)
- [10] Wang, Xiao-Li, Ke-Qin Zhu, and Shi-Zhu Wen. "On the performance of dynamically loaded journal bearings lubricated with couple stress fluids." *Tribology International* 35, no. 3 (2002): 185-191. [https://doi.org/10.1016/S0301-679X\(01\)00114-1](https://doi.org/10.1016/S0301-679X(01)00114-1)
- [11] Samyilingam, Lingenthiran, Navid Aslfattahi, Chee Kuang Kok, Kumaran Kadirgama, Norazlianie Sazali, Kia Wai Liew, Michal Schmirler et al. "Enhancing Lubrication Efficiency and Wear Resistance in Mechanical Systems through the Application of Nanofluids: A Comprehensive Review." *Journal of Advanced Research in Micro and Nano Engineering* 16, no. 1 (2024): 1-18. <https://doi.org/10.37934/armne.16.1.118>
- [12] Ideris, Muhammad Haziq, Shafie Kamaruddin, Mohd Hafis Sulaiman, Nor Aiman Sukindar, Ahmad Zahirani Ahmad Azhar, and Ahmad Shah Hizam Md Yasir. "Effects of Coating and Lubrication on Friction and Wear for Metal-to-Metal Application." *Journal of Advanced Research in Applied Mechanics* 110, no. 1 (2023): 52-62. <https://doi.org/10.37934/aram.110.1.5262>
- [13] Ismail, Mohd Farid, Wan Hamzah Azmi, Rizalman Mamat, and Abdul Hamid Hamisa. "Experimental Investigation on Newtonian Behaviour and Viscosity of TiO₂/PVE Nanolubricants for Application in Refrigeration System." *Journal of Advanced Research in Fluid Mechanics and Thermal Sciences* 92, no. 1 (2022): 9-17. <https://doi.org/10.37934/arfmts.92.1.917>
- [14] Huo, Jiaofei, Guangpeng Zhang, Aria Ghabussi, and Mostafa Habibi. "Bending analysis of FG-GPLRC axisymmetric circular/annular sector plates by considering elastic foundation and horizontal friction force using 3D-poroelasticity theory." *Composite Structures* 276 (2021): 114438. <https://doi.org/10.1016/j.compstruct.2021.114438>
- [15] Ghabussi, Aria, Mina Mortazavi, and Raghu Betha. "Seismic performance of a cold-formed and hot-rolled steel wall system equipped with curved steel dampers." In *Structures*, vol. 53, pp. 296-316. Elsevier, 2023. <https://doi.org/10.1016/j.istruc.2023.04.053>
- [16] Zhang, Liang, Zhengxian Chen, Mostafa Habibi, Aria Ghabussi, and Rayed Alyousef. "Low-velocity impact, resonance, and frequency responses of FG-GPLRC viscoelastic doubly curved panel." *Composite Structures* 269 (2021): 114000. <https://doi.org/10.1016/j.compstruct.2021.114000>
- [17] Al-Furjan, M. S. H., Mostafa Habibi, Aria Ghabussi, Hamed Safarpour, Mehran Safarpour, and Abdelouahed Tounsi. "Non-polynomial framework for stress and strain response of the FG-GPLRC disk using three-dimensional refined higher-order theory." *Engineering Structures* 228 (2021): 111496. <https://doi.org/10.1016/j.engstruct.2020.111496>
- [18] Safarpour, Mehran, Aria Ghabussi, Farzad Ebrahimi, Mostafa Habibi, and Hamed Safarpour. "Frequency characteristics of FG-GPLRC viscoelastic thick annular plate with the aid of GDQM." *Thin-Walled Structures* 150 (2020): 106683. <https://doi.org/10.1016/j.tws.2020.106683>

- [19] Munshi, Mohmmadraiyan M., A. R. Patel, and G. M. Deheri. "Effect of slip velocity on a magnetic fluid based squeeze film in rotating transversely rough curved porous circular plates." *Industrial Engineering Letters* 7, no. 8 (2017): 28-42.
- [20] Salma, A., and B. N. Hanumagowda. "Erratum to "Effect of MHD and viscosity variation on the couplestress squeeze film between curved circular plate and a flat porous plate" [Partial Differ. Equ. Appl. Math. 6 (2022) 100424]." *Partial Differential Equations in Applied Mathematics* 7 (2023): 100482. <https://doi.org/10.1016/j.padiff.2022.100482>
- [21] Hanumagowda, B. N., Tesymol Cyriac, H. S. Doreswamy, and A. Salma. "Analysis of static and dynamic characteristics of Secant slider bearing with MHD and couple stress fluid." *Malaya Journal of Matematik* 8, no. 02 (2020): 581-587. <https://doi.org/10.26637/MJM0802/0045>
- [22] Jyothi, V., B. N. Hanumagowda, and Amit Verma. "Analysis of pressure load-carrying capacity and squeezing time on magnetohydrodynamic couple stress fluid flow between sphere and flat plate with slip velocity." *International Journal of Modern Physics B* 38, no. 26 (2024): 2450349. <https://doi.org/10.1142/S0217979224503491>
- [23] Suresha, R., R. Arunkumar, B. N. Hanumagowda, Dilsora Abduvalieva, Nainaru Tarakaramu, Fuad A. Awwad, Emad A. A. Ismail, and M. Ijaz Khan. "Combined effect of magneto hydrodynamics, couple stress, and viscosity variation on squeeze film characteristics of a cylinder and rough flat plate." *SN Applied Sciences* 5, no. 12 (2023): 350. <https://doi.org/10.1007/s42452-023-05588-1>
- [24] Devakar, M., K. Ramesh, and K. Vajravelu. "Magnetohydrodynamic effects on the peristaltic flow of couple stress fluid in an inclined tube with endoscope." *Journal of Computational Mathematics and Data Science* 2 (2022): 100025. <https://doi.org/10.1016/j.jcmds.2022.100025>
- [25] Nabhani, Mohamed, and Mohamed El Khlifi. "Inertial MHD couple stress effects on infinitely wide slider bearings." *Tribology Transactions* 58, no. 2 (2015): 374-383. <https://doi.org/10.1080/10402004.2014.973544>
- [26] Sahraoui, Melik, and Massoud Kaviany. "Slip and no-slip velocity boundary conditions at interface of porous, plain media." *International Journal of Heat and Mass Transfer* 35, no. 4 (1992): 927-943. [https://doi.org/10.1016/0017-9310\(92\)90258-T](https://doi.org/10.1016/0017-9310(92)90258-T)
- [27] Ahmad, N., and J. P. Singh. "Magnetic fluid lubrication of porous-pivoted slider bearings with slip velocity." *Proceedings of the Institution of Mechanical Engineers, Part J: Journal of Engineering Tribology* 221, no. 5 (2007): 609-613. <https://doi.org/10.1243/13506501JET272>
- [28] Yang, Qin, Haijun Zhang, and Yulu Liu. "Improved modified Reynolds equation for thin-film gas lubrication from an extended slip velocity boundary condition." *Microsystem Technologies* 22 (2016): 2869-2875. <https://doi.org/10.1007/s00542-015-2667-4>
- [29] Shah, Rajesh C., and M. V. Bhat. "Lubrication of porous parallel plate slider bearing with slip velocity, material parameter and magnetic fluid." *Industrial Lubrication and Tribology* 57, no. 3 (2005): 103-106. <https://doi.org/10.1108/00368790510595066>
- [30] Guo, L., P. L. Wong, and F. Guo. "Effects of viscosity and sliding speed on boundary slippage in thin film hydrodynamic lubrication." *Tribology International* 107 (2017): 85-93. <https://doi.org/10.1016/j.triboint.2016.11.021>
- [31] Ahmad, N., and J. P. Singh. "Porous pivoted slider bearings lubricated with a couple stress fluid." *Proceedings of the Institution of Mechanical Engineers, Part J: Journal of Engineering Tribology* 220, no. 7 (2006): 639-642. <https://doi.org/10.1243/13506501J10105>
- [32] Jayaprakash, J., Vedyappan Govindan, Jagadiash Patil, Bannihalli N. Hanumagowda, Hijaz Ahmad, and Jagadish V. Tawade. "The Effect of Magneto-hydrodynamics on Curved Circular Plate and Porous-rough Flat Plate with Non-Newtonian Fluid." *Journal of Applied and Computational Mechanics* 10, no. 3 (2024): 584-596.
- [33] Cyriac, Tesymol, B. N. Hanumagowda, M. Umeshaiyah, Vijaya Kumar, Jasgurpreet Singh Chohan, R. Naveen Kumar, and K. Karthik. "Performance of rough secant slider bearing lubricated with couple stress fluid in the presence of magnetic field." *Modern Physics Letters B* 38, no. 19 (2024): 2450140. <https://doi.org/10.1142/S0217984924501409>
- [34] Vinutha, R., B. N. Hanumagowda, and K. R. Vasanth. "Theoretical analysis of effect of MHD, couple stress and slip velocity on squeeze film lubrication characteristics of Long Cylinder and Infinite Rough Plate." *Tribology International* 191 (2024): 109164. <https://doi.org/10.1016/j.triboint.2023.109164>